Ursolic acid inhibits colorectal cancer angiogenesis through suppression of multiple signaling pathways

JIUMAO LIN[1,2], YOUQIN CHEN[3], LIHUI WEI[1,2], ZHENFENG HONG[1], THOMAS J. SFERRA[3] and JUN PENG[1,2]

[1]Academy of Integrative Medicine Biomedical Research Center and [2]Fujian Key Laboratory of Integrative Medicine on Geriatrics, Fujian University of Traditional Chinese Medicine, Minhou Shangjie, Fuzhou, Fujian 350122, P.R. China; [3]Rainbow Babies and Children's Hospital, Case Western Reserve University School of Medicine, Cleveland, OH 44106, USA

Received July 19, 2013; Accepted September 2, 2013

DOI: 10.3892/ijo.2013.2101

Abstract. Angiogenesis plays a critical role in the development of solid tumors by supplying nutrients and oxygen to support continuous growth of tumor as well as providing an avenue for hematogenous metastasis. Tumor angiogenesis is highly regulated by multiple intracellular signaling transduction cascades such as Hedgehog, STAT3, Akt and p70S6K pathways that are known to malfunction in many types of cancer including colorectal cancer (CRC). Therefore, suppression of tumor angiogenesis through targeting these signaling pathways has become a promising strategy for cancer chemotherapy. Ursolic acid (UA) is a major active compound present in many medicinal herbs that have long been used in China for the clinical treatment of various types of cancer. Although previous studies have demonstrated an antitumor effect for UA, the precise mechanisms of its anti-angiogenic activity are not well understood. To further elucidate the mechanism(s) of the tumorcidal activity of UA, using a CRC mouse xenograft model, chick embryo chorioallantoic membrane (CAM) model, the human colon carcinoma cell line HT-29 and human umbilical vein endothelial cells (HUVECs), in the present study we evaluated the efficacy of UA against tumor growth and angiogenesis *in vivo* and *in vitro* and investigated the underlying molecular mechanisms. We found that administration of UA significantly inhibited tumor volume but had no effect on body weight changes in CRC mice, suggesting that UA can suppress colon cancer growth *in vivo* without noticeable signs of toxicity. In addition, UA treatment reduced intratumoral microvessel density (MVD) in CRC mice, decreased the total number of blood vessels in the CAM model, and dose and time-dependently inhibited the proliferation, migration and tube formation of HUVECs, demonstrating UA's antitumor angiogenesis *in vivo* and *in vitro*. Moreover, UA treatment inhibited the expression of critical angiogenic factors, such as VEGF-A and bFGF. Furthermore, UA suppressed the activation of sonic hedgehog (SHH), STAT3, Akt and p70S6K pathways. Collectively, our findings suggest that inhibition of tumor angiogenesis via suppression of multiple signaling pathways might be one of the mechanisms whereby UA can be effective in cancer treatment.

Correspondence to: Dr Jun Peng, Academy of Integrative Medicine, Fujian University of Traditional Chinese Medicine, 1 Huatuo Road, Minhou Shangjie, Fuzhou, Fujian 350122, P.R. China
E-mail: pjunlab@hotmail.com

Abbreviations: UA, ursolic acid; CRC, colorectal cancer; CAM, chorioallantoic membrane; HUVEC, human umbilical vein endothelial cell; DMSO, dimethyl sulfoxide; MTT, 3-(4,5-dimethyl-thiazol-2-yl)-2,5-diphenyltetrazolium bromide; IHC, immunohistochemical staining; VEGF, vascular endothelial growth factor; bFGF, basic fibroblast growth factor; MVD, microvessel density; SHH, sonic hedgehog signal pathway; STAT3, signal transducer and activator of transcription 3; Akt, AKT8 in rodent T-cell lymphoma; p70S6K, p70S6 kinase

Key words: tumor angiogenesis, ursolic acid, signal pathway

Introduction

Colorectal cancer (CRC) is one of the most common human malignant cancers with over one million new cases and more than a half million deaths around the world each year (1). To date, chemotherapy remains one of the main therapeutic approaches for advanced CRC; and 5-fluorouracil (5-FU)-based regimens are considered as standard chemotherapeutics (2,3). However, due to drug resistance and toxicity against normal tissues, systemic chemotherapy using 5-FU-based regimens produces objective response rates of <10-20% (2,4-6). These problems limit the effectiveness of current CRC chemotherapy, highlighting the urgent need for the development of novel antitumor agents.

Angiogenesis, a process involving the growth of new blood vessels from the pre-existing vasculature (7,8), is essential in various human biological processes including wound healing, reproduction and embryonic development (9-11). However, dyregulation of angiogenesis also plays a critical role in the development of solid tumors, supplying nutrients and oxygen to support continuous growth of tumor as well as providing an avenue for hematogenous metastasis (11-13). Tumor angiogenesis is highly regulated by multiple intracellular signaling transduction cascades such as Hedgehog, signal transducer and activator of transcription 3 (STAT3), Akt and p70S6 kinase (p70S6K) pathways that are known to malfunction in many

types of cancer. The Hedgehog (HH) signaling pathway is important for embryonic development (14); its aberrant activation has been associated with many human cancers including CRC (15-19). Mammals have three Hedgehog homologues (Sonic Hedgehog, Indian Hedgehog and Desert Hedgehog), of which Sonic Hedgehog (SHH) is the best studied. Activation of HH signaling is initiated by binding of Hh to the transmembrane receptor Patched (Ptch). This results in the release of Ptch-mediated suppression of Smoothened (Smo). Smo subsequently activates the Gli family of transcription factors that regulate the expression of various angiogenic mediators promoting angiogenesis (20-23). STAT3 plays an essential role in cell survival, proliferation and angiogenesis (24). After activation via phosphorylation, STAT3 proteins in the cytoplasm dimerize and translocate to the nucleus where they regulate the expression of critical genes involved in cancer progression. Constitutive activation of STAT3 is strongly associated with cancer development and commonly suggests a poor prognosis (25,26). PI3K-dependent Akt pathway is essential for cell proliferation and survival and has been shown to be activated in several cancer types (27-29). After activation by extracellular stimuli, PI3K is able to phosphorylate PI(4)P and PI(4,5) P2 to generate PI(3,4)P2 and PI(3,4,5)P3, respectively. These lipids serve as plasma membrane docking sites for proteins containing pleckstrin-homology (PH) domains, such as Akt and its upstream activator 3-phosphoinositide-dependent protein kinase-1 (PDK1). The colocalization of PDK1 and Akt in plasma membrane results in the phosphorylation of Akt, which in turn activates mTOR (mammalian target of rapamycin) leading to the phosphorylation/activation of p70S6K. The Akt-mTOR-p70S6K signaling pathway is considered as a central regulatory pathway involved in the regulation of cell proliferation, differentiation, survival and angiogenesis (30-33). Therefore, inhibition of angiogenesis via modulation of these signalings has become a major focus for anticancer drug development.

Due to drug resistance and cytotoxicity of currently-used chemotherapies, natural products, including traditional Chinese medicine (TCM), have received great interest since they have relatively few side-effects as compared to modern chemotherapeutics and have been used for thousands of years as important alternative remedies for various diseases including cancer (34,35). Thus, identifying naturally occurring agents is a promising approach for anticancer treatment. Ursolic acid (UA), a pentacyclic triterpene acid, is a biologically active compound present in many traditional Chinese medicinal herbs, such as *Hedyotic diffusa, Spica prunellae, Patrinia scabiosaefolia* and *Scutellaria barbata* that have long been used in China for the clinical treatment of CRC (36-39). Previous studies report that UA exhibits a broad range of pharmacological properties such as anti-inflammatory, antiviral, antioxidant, hepatoprotective, cytotoxic, antitumor, anti-angiogenesis, and anti-metastatic activities (40). Recent studies have shown that UA inhibits the proliferation and induces apoptosis and/inhibits proliferation of colon carcinoma cells (13,41-43). In order to further elucidate the mechanism of tumorcidal activity of UA, in the present study we evaluated its effect on CRC growth and angiogenesis *in vivo* and *in vitro*, and investigated the underlying molecular mechanisms of its action.

Materials and methods

Materials and reagents. Usolic acid (UA) was purchased from Sigma-Aldrich Chemical (St. Louis, MO, USA). Matrigel was provided by Becton-Dickinson (San Jose, CA, USA). Roswell Park Memorial Institute medium-1640 (RPMI-1640), Dulbecco's modified Eagle's medium (DMEM), fetal bovine serum (FBS), penicillin-streptomycin, trypsin-EDTA and TRIzol reagent were purchased from Invitrogen (Carlsbad, CA, USA). SuperScript II reverse transcriptase was obtained from Promega (Madison, WI, USA). The *In Vitro* Angiogenesis Assay kit was purchased from Millipore (Billerica, MA, USA). Human VEGF-A and bFGF ELISA kits were obtained from Shanghai Xitang Biological Technology Ltd. (Shanghai, China). All antibodies were purchased from Santa Cruz Biotechnology (Santa Cruz, CA, USA). BCA Protein assay kit was purchased from Tiangen Biotech (Beijing) Co., Ltd. Bio-Plex phosphoprotein assay kits were purchased from Bio-Rad (Hercules, CA, USA). All other chemicals, unless otherwise stated, were obtained from Sigma-Aldrich (St. Louis, MO, USA).

Cell culture. Human colon carcinoma HT-29 cells were obtained from the Cell Bank of Chinese Academy of Sciences (Shanghai, China). Human umbilical vein endothelial cells (HUVECs) were purchased from Xiangya Cell Center, University of Zhongnan (Hunan, China). HT-29 cells and HUVECs were grown in DMEM and RPMI-1640, respectively. Both DMEM and RPMI-1640 were supplemented with 10% (v/v) FBS, 100 U/ml penicillin, and 100 μg/ml streptomycin. All cell lines were cultured at 37˚C, 5% CO_2 and in a humidified environment.

Animals. Male BALB/c athymic (nude) mice (with an initial body weight of 20-22 g) were obtained from Shanghai SLAC Laboratory Animal Co., Ltd. (Shanghai, China) and housed under pathogen-free conditions with controlled temperature (22˚C), humidity, and a 12-h light/dark cycle. Food and water were given *ad libitum* throughout the experiment. All animal treatments were performed strictly in accordance with international ethical guidelines and the National Institutes of Health Guide concerning the Care and Use of Laboratory Animals. The experiments were approved by the Institutional Animal Care and Use Committee of Fujian University of Traditional Chinese Medicine.

In vivo nude mouse xenograft study. CRC xenograft mice were produced with HT-29 cells. The cells were grown in culture and then detached by trypsinization, washed, and resuspended in serum-free DMEM. Resuspended cells ($1.5x10^6$) mixed with Matrigel (1:1) were subcutaneously injected into the right flank of mice to initiate tumor growth. At 5 days following xenograft implantation (tumor size ~3 mm in diameter), mice were randomized into two groups (n=10) and treated with UA (dissolved in PBS) 12.5 mg/kg or saline by daily intraperitoneal injection, 6 days a week for 16 days. Body weight and tumor size were measured. Tumor size was determined by measuring the major (L) and minor (W) diameter with a caliper. The tumor volume was calculated according to the following formula: tumor volume = $\pi/6 \times L \times W^2$. At the end

of the experiment, the animals were anaesthetized with pelltobarbitalum natricum, and tumors were excised. A portion of each tumor was fixed in 10% buffered formalin and the remaining tissue snap-frozen in liquid nitrogen and stored at -80˚C.

Immunohistochemistical analysis of CRC tumor tissues. Six tumors were randomly selected from UA-treatment or control groups. Tumor tissues were fixed in 10% formaldehyde for 12 h, paraffin-embedded, sectioned and placed on slides. The slides were subjected to antigen retrieval and endogenous peroxidase activity was quenched with hydrogen peroxide. Non-specific binding was blocked with normal serum in PBS (0.1% Tween-20). Rabbit polyclonal antibodies against CD31, SHH, Gli-1, VEGF-A and bFGF (all in 1:200 dilution, Santa Cruz Biotechnology) were used to detect the relevant proteins. The binding of the primary antibody was demonstrated with a biotinylated secondary antibody, horseradish peroxidase (HRP)-conjugated streptavidin (Dako) and diaminobenzidine (DAB) as the chromogen. The tissues were counterstained with diluted Harris hematoxylin. After staining, five high-power fields (at magnification of x400) were randomly selected in each slide. The proportion of positive cells in each field was determined using the true color multi-functional cell image analysis management system (Image-Pro Plus, Media Cybernetics, USA). To control for non-specific staining, PBS was used to replace the primary antibody as a negative control.

Chick chorioallantoic membrane (CAM) assay. A CAM assay was performed to determine the *in vivo* anti-angiogenic activity of UA. Briefly, 10 μl of UA (25 μg/μl) was loaded onto a 0.5-cm diameter Whatman filter paper. The filter was then applied to the CAM of a 7-day embryo. After incubation for 72 h at 37˚C, the region surrounding the filter was photographed with a digital camera. The number of blood vessels was quantified manually in a circular perimeter surrounding the implants, at a distance of 0.25 cm from the edge of the filter. Assays were performed twice with a final total of 10 eggs for each data point.

Cell viability evaluation by MTT assay. UA was dissolved in DMSO and diluted to working concentrations with culture medium. The final concentration of DMSO in the medium for all cell-based experiments was 0.1% HUVECs were seeded into 96-well plates at a density of $1.0x10^4$ cells/well in 0.1 ml medium and incubated at 37˚C under a 5% CO_2 for 24 h. The cells were treated with various concentrations of UA for 24 h or with 40 μM of UA for different periods of time. Treatment with 0.1% DMSO was included as the vehicle control. At the end of the treatment, 10 μl MTT [5 mg/ml in phosphate buffered saline (PBS)] were added to each well, and the samples were incubated for an additional 4 h at 37˚C. The purple-blue MTT formazan precipitate was dissolved in 100 μl DMSO. Absorbance was measured at 570 nm using an ELISA reader (BioTek, Model EXL800, USA).

Migration assay of HUVECs. Migration of HUVECs was performed by the wound healing method. HUVECs were seeded into 12-well plates at a density of $2x10^5$ cells/well in 1 ml medium. After 24 h of incubation, cells were scraped away vertically in each well using a P100 pipette tip. Three randomly selected views along the scraped line were photographed in each well using phase-contrast inverted microscopy at a magnification of x100. Cells were treated with various concentrations of UA for 24 h, and a second set of images were taken using the same method. A reduction in the size of the scraped region is indicative of cell migration.

Tube formation assay of HUVECs. HUVEC tube formation was examined using the ECMatrix assay kit (Millipore) following the manufacturer's instructions. Briefly, confluent HUVECs were harvested and diluted ($1x10^4$ cells) in 50 μl of medium containing various concentrations of UA. The harvested cells were seeded with ECMatrix gel (1:1 v/v) into 96-well plates and incubated for 9 h at 37˚C. The cells were photographed using phase-contrast inverted microscopy at a magnification of x100. The level of HUVEC tube formation was quantified by calculating the length of the tubes in three randomly chosen fields from each well.

RT-PCR. Total RNA was isolated from tumor tissues (three tumors were randomly selected from UA-treatment or control groups) or HT-29 cells with TRIzol reagent. Oligo(dT)-primed RNA (1 μg, isolated from tumor tissues or cells) was reverse-transcribed with SuperScript II reverse transcriptase (Promega) according to the manufacturer's instructions. The obtained cDNA was used to determine the level of VEGF-A, bFGF, Shh and Gli-1 mRNA by PCR with Taq DNA polymerase (Fermentas). GAPDH was used as an internal control. Samples were analyzed by gel electrophoresis (1.5% agarose). The DNA bands were examined using a gel documentation system (Model Gel Doc 2000, Bio-Rad).

Western blot analysis. HT-29 cells ($2.5x10^5$) in 5 ml medium were seeded into 25 cm^2 flasks and treated with the indicated concentrations of UA for 24 h. Treated cells were lysed in mammalian cell lysis buffer (M-PER, Thermo Scientific, Rockford, IL, USA) containing protease (EMD Biosciences) and phosphatase inhibitor (Sigma-Aldrich) cocktails and centrifuged at 14,000 x g for 15 min. Protein concentrations in cell lysate supernatants were determined by BCA protein assay. Equal amounts of protein from each tumor or cell lysate were resolved on 12% Tris-glycine gels and transferred onto PVDF membranes. The membranes were blocked for 2 h with 5% non-fat dry milk and incubated with the desired primary antibody directed against Shh, Gli-1, or β-actin (all in 1:1,000 dilutions) overnight at 4˚C. Appropriate HRP-conjugated secondary antibodies with chemiluminescence detection were used to image the antibody-detected proteins.

Bio-Plex Phosphoprotein assay. Eight tumors were randomly selected from UA-treatment or control groups and homogenized. For analysis of phosphorylation of Akt and p70S6K *in vitro*, HT-29 cells ($2.5x10^5$) were seeded into 25-cm^2 flasks in 5 ml medium and treated with 40 μM of UA for 24 h. To detect STAT3 phosphorylation *in vitro*, HT-29 cells were first grown in complete DMEM (10% FBS) until ~70% confluency and subsequently cultured in FBS-free medium overnight. The medium was replaced with DMEM with 10% FBS and cells were pre-treated with UA (40 μM) for 1 h followed by

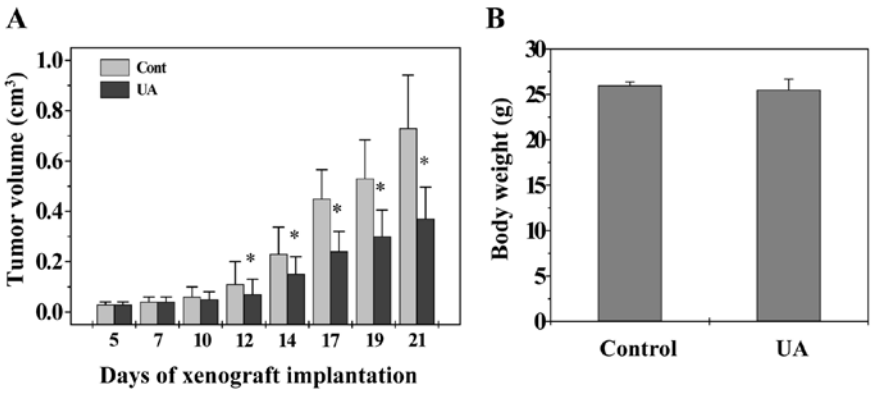

Figure 1. UA inhibits tumor growth in CRC xenograft mice. After tumor development, the mice were administered with 12.5 mg/kg of UA or saline daily by intraperitoneal injection, 6 days a week for 16 days. Tumor volume (A) and body weight (B) were measured. Data are averages with SD (error bars) from 10 individual mice in each group. *P<0.01, versus controls.

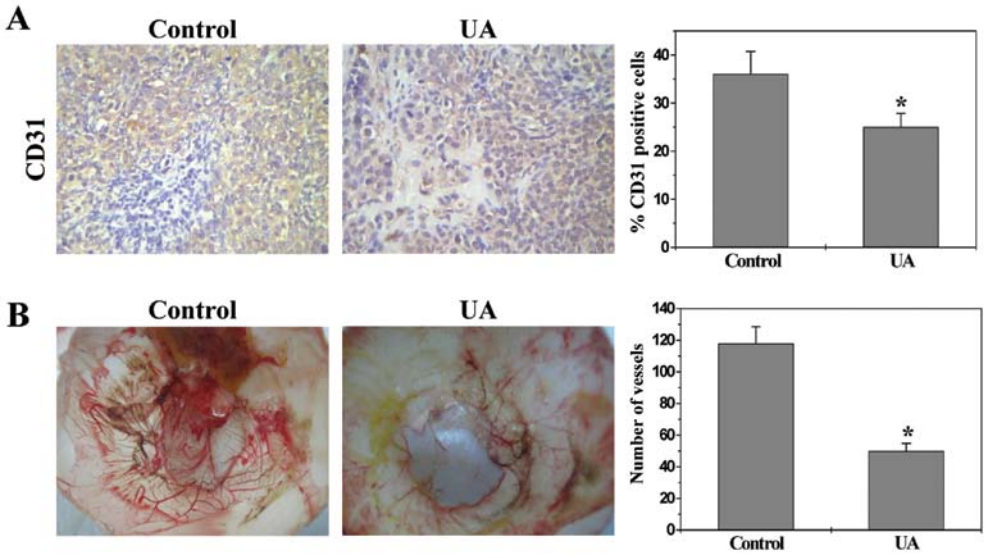

Figure 2. Effect of UA on angiogenesis in CRC xenograft mice and chick chorioallantoic membrane (CAM). (A) At the end of the study, tumor tissues were processed for immunohistochemical (IHC) staining for CD31. The photographs are representative images taken at a magnification of x400. Quantification of IHC assay was represented as percentage of positively-stained cells. Data shown are averages with SD (error bars) from 6 individual mice in each group. (B) UA anti-angiogenesis on the angiogenesis of chick chorioallantoic membrane (CAM). A 0.5-cm diameter filter paper loaded with or without 0.25 mg of UA was applied to the CAM and incubated at 37˚C for 72 h. The number of blood vessels was quantified. Assays were performed twice, containing in total 10 eggs for each data point. Representative images are shown. Data are averages with SD (error bars) from 10 eggs in each group. *P<0.01, versus controls.

stimulation with 10 ng/ml of IL-6 for 15 min. Tumor tissues and treated cells were lysed using a commercially available lysis kit (Bio-Rad Laboratories) and centrifuged at 14,000 x g for 15 min. Protein concentrations of the clarified supernatants were determined by BCA protein assay. The presence of p-STAT3, p-Akt and p-p70S6K was detected using a bead-based multiplex assay for phosphoproteins (Bio-Plex Phosphoprotein assay, Bio-Rad Laboratories) according to the manufacturer's protocol. Data were collected and analyzed using the Bio-Plex 200 suspension array system (Bio-Rad).

Measurement of VEGF-A and bFGF protein expression in HT-29 cells by ELISA. HT-29 cells were seeded into 6-well plates at a density of $2x10^5$ cells/well in 2 ml medium and treated with the indicated concentrations of UA for 24 h. The medium and cells from each well were collected and stored at -80˚C until analyzed. The level of VEGF-A or bFGF in the media was measured using an ELISA kit (Xitang Biological Technology Ltd.) according to the manufacturer's instructions. The concentrations of VEGF-A and bFGF were determined by comparison to serial dilutions of VEGF-A and bFGF purified standards.

Statistical analysis. Data are presented as the mean ± SD for the indicated number of independently performed experiments. The data were analyzed using the SPSS package for Windows (Version 17.0). Statistical analysis was carried out with Student's t-test and ANOVA. Differences with $P<0.05$ were considered to be statistically significant.

Results

UA inhibits tumor growth in colorectal cancer (CRC) xenograft mice. The *in vivo* efficacy of UA against tumor growth was evaluated by measuring tumor volume in CRC xenograft

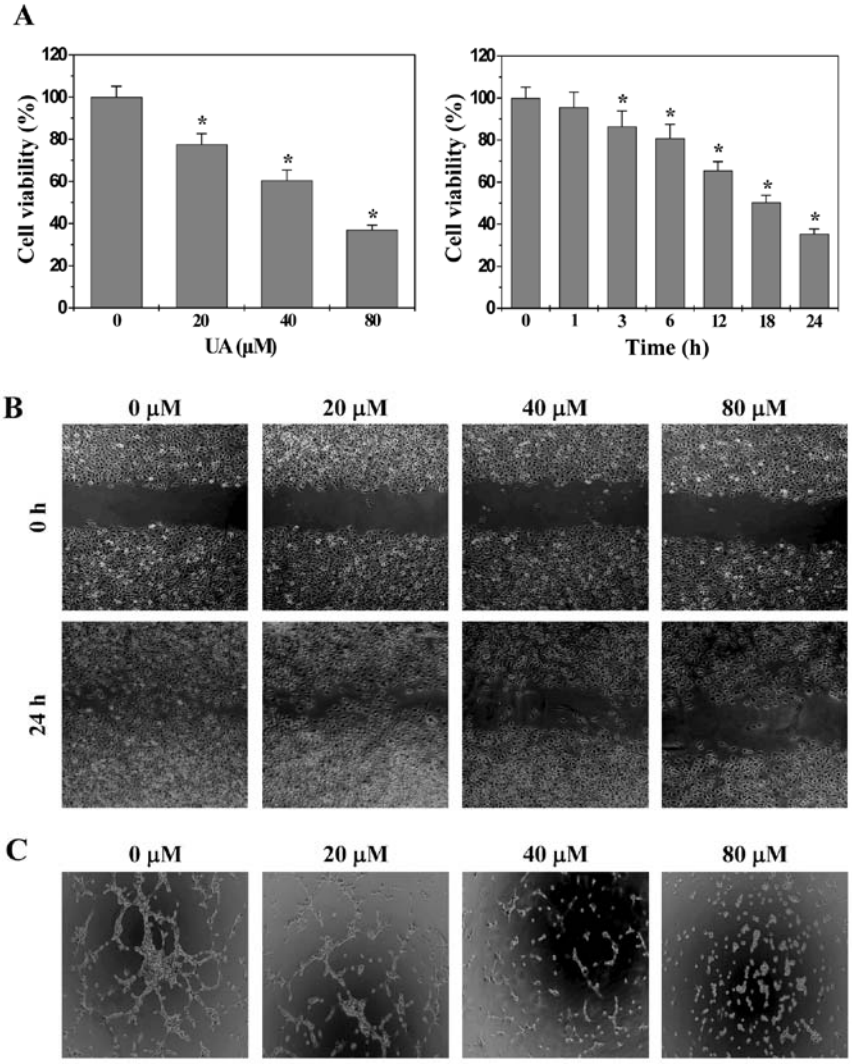

Figure 3. Effect of UA on angiogenesis in HUVECs. (A) Cells were treated with the indicated concentrations of UA for 24 h or with 40 μM of UA for the indicated time periods. Cell viability was determined by the MTT assay. The data were normalized to the viability of control cells (100%, treated with 0.1% DMSO vehicle). Data are averages with SD (error bars) from three independent experiments. (B) After treated with indicated concentrations of UA for 24 h, the migration pattern of HUVECs was observed using phase-contrast microscopy. The photographs were taken at a magnification of x100. Images are representative of three independent experiments. (C) HUVECs were harvested and diluted in medium containing various concentrations of UA. The harvested cells were then seeded 1:1 in ECMatrix gel (v/v) coated plates and incubated for 9 h at 37˚C. The network-like structures were examined by phase-contrast microscopy. The photographs were taken at a magnification of x100. Images are representative of three independent experiments.

mice. As shown in Fig. 1, administration of UA significantly inhibited tumor growth throughout the study, as compared with the control group (P<0.05), whereas the body weight gain in experimental animals was not affected by UA treatment, suggesting that UA is potent in suppressing colon tumor growth *in vivo*, without apparent adverse effects.

UA inhibits angiogenesis in vivo and in vitro. To determine the effect of UA on tumor angiogenesis, we examined the intratumoral microvessel density (MVD) in CRC mice by evaluating expression of the endothelial cell-specific marker CD31. Data from immunohistochemical staining (IHC) assay showed that the percentage of CD31-positive cells in control or UA-treated mice was 36.0±4.8 or 25.0±2.8%, respectively (Fig. 2A, P<0.01), demonstrating UA's inhibitory activity on tumor angiogenesis. The *in vivo* anti-angiogenic activity of UA was further confirmed using a chick chorioallantoic membrane (CAM) model. As shown in Fig. 2B, UA treatment significantly reduced the total number of blood vessels in chicken embryos as compared to untreated controls (P<0.01).

The processes of angiogenesis include endothelial cell (EC) proliferation, migration, and alignment into tubular structures. To evaluate the anti-angiogenic effect of UA we modeled each of these processes with HUVECs *in vitro*. As shown in Fig. 3A, UA treatment dose- and time-dependently decreased the proliferation (viability) of HUVECs compared to untreated control cells (P<0.01). In addition, UA treatment inhibited HUVEC migration after monolayer wounding (Fig. 3B). Moreover, we examined the effect of UA on capillary tube formation of HUVECs using an extracellular matrix, in which cultured ECs rapidly align and form hollow tube-like structures. As shown in Fig. 3C, untreated HUVECs formed elongated tube-like structures, whereas UA treatment resulted in a significant decrease in capillary tube formation (P<0.01). Taken together, these data suggested that UA-caused inhibition of colon tumor growth is accompanied by its anti-angiogenic activity.

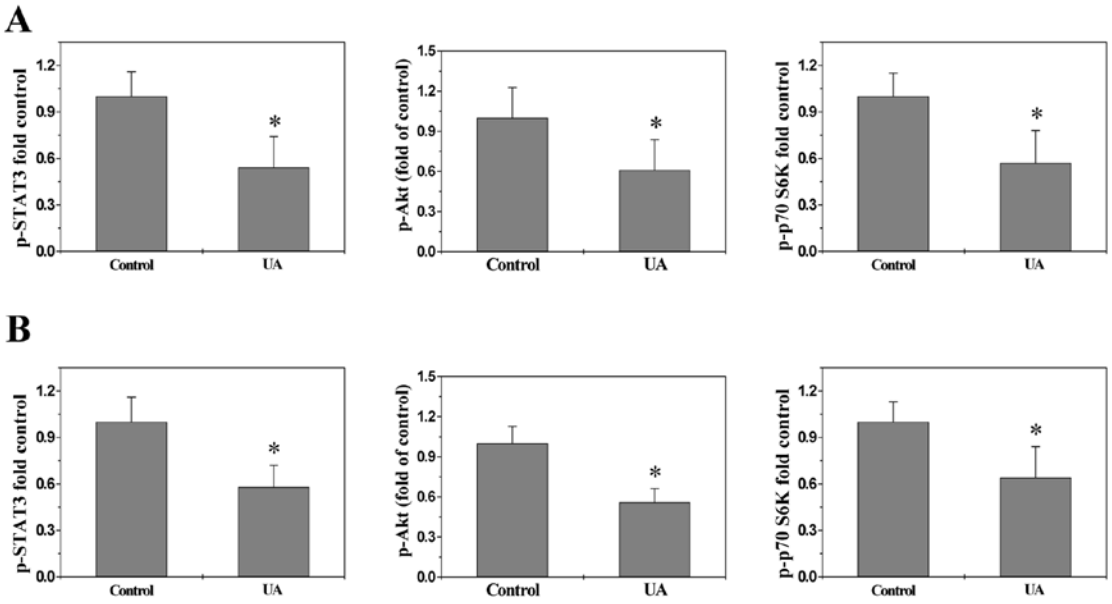

Figure 4. Effect of UA on phosphorylation of STAT3, Akt and p70S6K in CRC xenograft mice and HT-29 cells. The phosphorylation levels of STAT3, Ak and p70S6K in tumor tissues (A) and in HT-29 cells (B) were determined by Bio-Plex Phosphoprotein assay. The data were normalized to the phosphorylation level within controls and represented as fold of control. Data are averages with SD (error bars) from 8 mice in each group or three independent cell-based experiments. *P<0.01, versus controls.

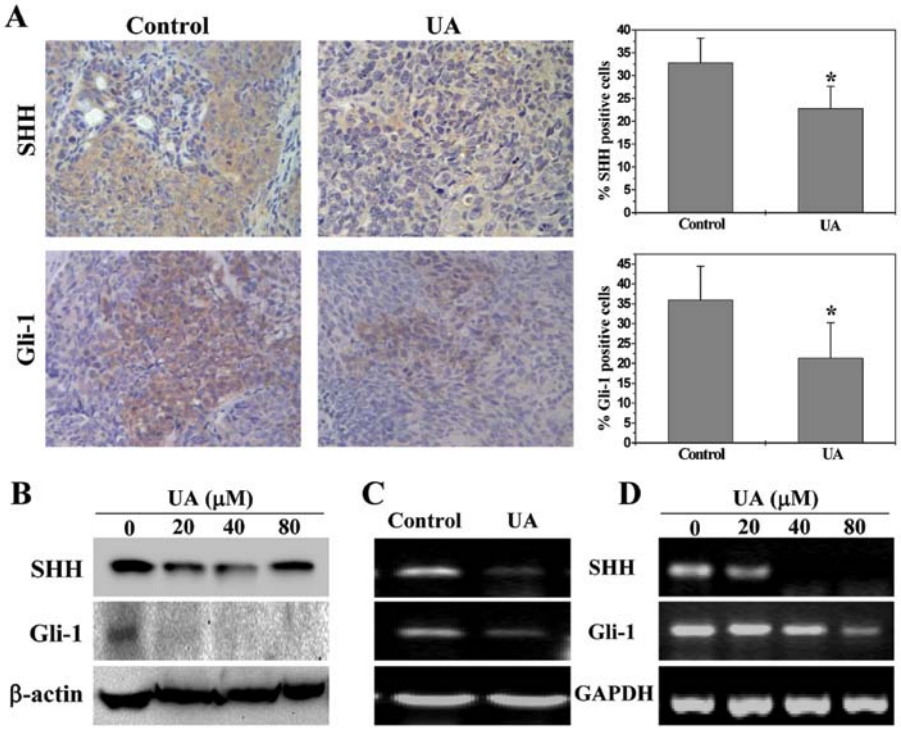

Figure 5. Effect of UA on the activation of Shh pathway in CRC xenograft mice and HT-29 cells. (A) Protein expression of Shh and Gli-1 in tumor tissues was determined by IHC assay. Images are representative and quantification data are averages with SD (error bars) from 6 mice in each group. *P<0.01, versus controls. (B) The protein expression levels of Shh and Gli-1 in HT-29 cells were determined by western blotting. β-actin was used as the internal control. The mRNA levels of Shh and Gli-1 in tumor tissues (C) or in HT-29 cells (D) were determined by RT-PCR. GAPDH was used as the internal control. Images of western blotting and RT-PCR are representative of 3 mice in each group or three independent cell-based experiments.

UA suppresses multiple signaling pathways in vivo and in vitro. To explore the underlying mechanisms of anti-angiogenic activities of UA, we determined its effect on the activation of several CRC-related signal transduction cascades. Activation of STAT3, Akt and p70S6K is mediated by its phosphorylation, we therefore investigated the effect of UA on STAT3, Akt and p70S6K activation in CRC xenograft tumor tissues and HT-29 cells by Bio-Plex Phosphoprotein assay. We found after UA treatment the phosphorylation level of STAT3, Akt and p70S6K in both tumors (Fig. 4A) and HT-29 cells (Fig. 4B) was

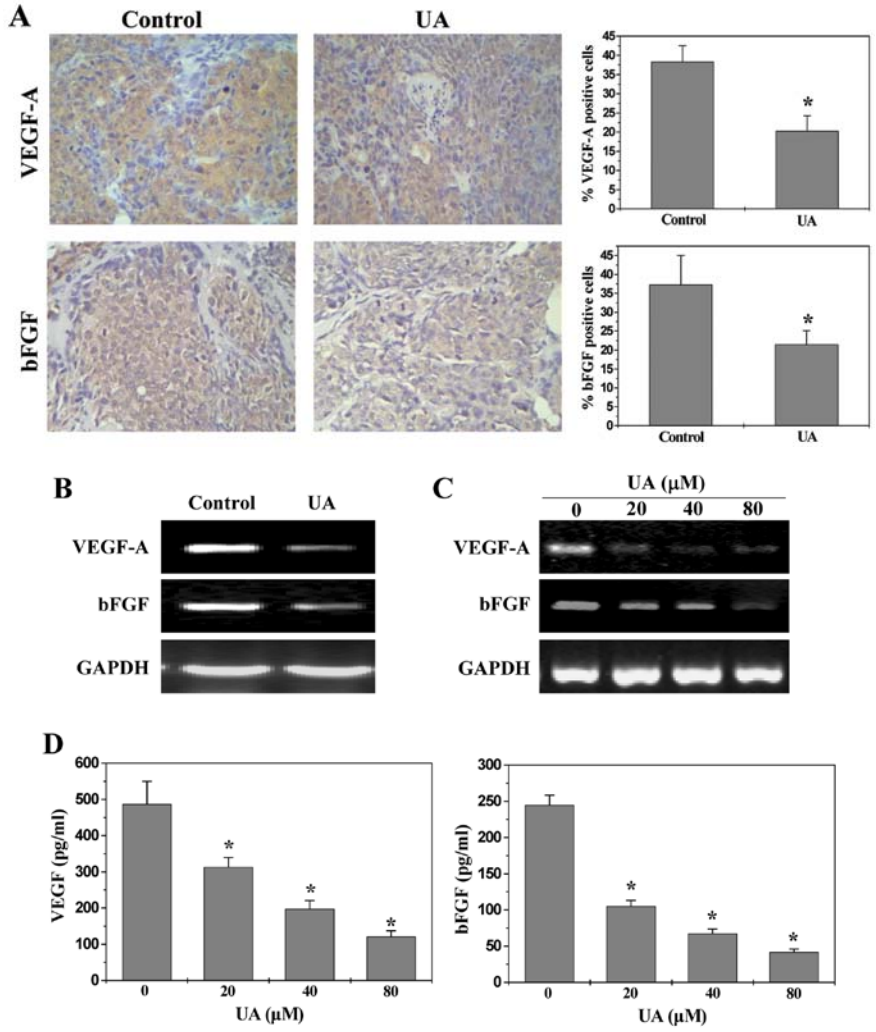

Figure 6. Effect of UA on the expression of VEGF-A and bFGF in CRC xenograft mice and HT-29 cells. (A) Protein expression of VEGF-A and bFGF in tumor tissues was determined by IHC assay. Images are representative and quantification data are averages with SD (error bars) from 6 mice in each group. *P<0.01, versus controls. The mRNA levels of VEGF-A and bFGF in tumor tissues (B) or in HT-29 cells (C) were determined by RT-PCR. GAPDH was used as the internal control. Images are representative of 3 mice in each group or three independent cell-based experiments. (D) The secretion levels of VEGF-A and bFGF in HT-29 cells were determined by ELISA. Data are averages with SD (error bars) from three independent experiments. *P<0.01, versus controls.

decreased as compared to controls (P<0.01). The activation of SHH pathway was evaluated by examining the expression of the key mediators of SHH pathway in CRC xenograft tumors and HT-29 cells. As shown in Fig. 5A, the percentage of cells in the CRC xenograft tumors expressing SHH and Gli-1 in the control group was 32.8±5.3 and 36.0±8.4%, respectively, whereas the levels in UA-treated mice were 22.8±4.8 and 21.3±8.9%, respectively (P<0.01). Similarly, UA treatment significantly reduced the protein expression of SHH and Gli-1 in HT-29 cells (Fig. 5B). Data from RT-PCR showed that the pattern of mRNA expression was similar to their respective protein levels (Fig. 5C and D). Collectively, these data suggest that UA significantly suppresses the activation of multiple signaling pathways mediating tumor angiogenesis.

UA inhibits the expression of VEGF-A and bFGF. VEGF-A and bFGF are critical target gene of the above-mentioned pathways (30,31,43,44). As most potent angiogenic stimulators, VEGF-A and bFGF are commonly overexpressed in many kinds of human cancer correlating with tumor progression and poorer prognosis (45-48). To further investigate the mechanism whereby UA inhibited angiogenesis, we determined its effect on VEGF-A and bFGF expression. Data from RT-PCR, IHC and ELISA analyses indicated that UA treatment profoundly decreased mRNA and protein levels of VEGF-A and bFGF in both CRC xenograft tumor tissues and HT-29 cells (Fig. 6).

Discussion

Due to its essential role in the growth, progression and metastasis of solid tumors, angiogenesis has become an attractive target for anticancer chemotherapy. A variety of anti-angiogenic agents is currently in preclinical development, with some of them now entering clinical trials. However, the administration of angiogenesis inhibitors may cause cardiovascular complications, including impaired wound healing, bleeding, hypertension, proteinuria and thrombosis (45-48), due to their intrinsic cytotoxicity against non-tumor associated endothelial cells. In addition, since multiple signaling pathways are involved in the

process of tumor angiogenesis, most currently-used angiogenic inhibitors, which typically are designed to affect a single target, may be insufficient and probably lead to resistance (49). These problems highlight the urgent need for the development of multi-target agents with minimal side effects and toxicity. Natural products have received great interest since they have relatively fewer side effects as compared to modern chemotherapeutics and have been shown to display multiple therapeutic effects for various diseases including cancer. Ursolic acid (UA), a major active compound of many traditional Chinese medicinal herbs, has been shown to possess anticancer activity. However, the precise mechanism of its potential tumoricidal activity remains largely unclear. Therefore, before UA can be further developed as an anticancer agent, the mode of action for its antitumor effects should be fully elucidated.

In the present study, using a CRC mouse xenograft model we demonstrated that UA could inhibit cancer growth *in vivo*, without apparent sign of toxicity. In addition, we found that UA significantly reduced the intratumoral microvessel density (MVD) in CRC xenograft mice and the total number of blood vessels in chick chorioallantoic membrane, suggesting that that UA-caused inhibition of colon tumor growth may be associated with its anti-angiogenic activity. Moreover, using human umbilical vein endothelial cells (HUVEC), we found that UA dose- and/or time-dependently inhibited several typical features of angiogenic process, i.e. suppressing endothelial cell proliferation, inhibiting migration and capillary tube formation of endothelial cells, further demonstrating the anti-angiogenic activity of UA.

Tumor angiogenesis is tightly regulated by multiple signal transduction cascades including SHH, STAT3 and Akt pathways. Activation of these signals upregulates the expression of various angiogenic factors including VEGF-A and bFGF which exert pro-angiogenic function via binding to their specific receptors located on vascular endothelial cells (36,50,51), eventually promoting angiogenesis. In this study we found that UC treatment inhibited the activation of STAT3, Akt and SHH pathways both *in vivo* in CRC tumors and *in vitro* in human colon carcinoma HT-29 cells since UA significantly suppressed the phosphorylation of STAT3, Akt and p70S6K, as well as the mRNA and protein expression of the key mediators of SHH signaling. Consistently, UA treatment profoundly downregulated the expression of VEGF-A and bFGF in both CRC tumors and HT-29 cells.

In conclusion, here we proposed that inhibition of tumor angiogenesis via suppression of multiple signaling pathways might be one of the mechanisms whereby UA can be effective in cancer treatment.

Acknowledgements

This study was supported by the National Natural Science Foundation of China (no. 81073097).

References

1. Jemal A, Bray F, Center MM, Ferlay J, Ward E and Forman D: Global cancer statistics. CA Cancer J Clin 61: 69-90, 2011.
2. Gustin DM and Brenner DE: Chemoprevention of colon cancer:current status and future prospects. Cancer Metastasis Rev 21: 323-348, 2002.
3. Lin JM, Chen YQ, Wei LH, Chen XZ, Xu W, Hong ZF, Sferra TJ and Peng J: *Hedyotis Diffusa* Willd extract induces apoptosis via activation of the mitochondrion-dependent pathway in human colon carcinoma cells. Int J Oncol 37: 1331-1338, 2010.
4. Van Cutsem E and Costa F: Progress in the adjuvant treatment of colon cancer: has it influenced clinical practice? JAMA 294: 2758-2760, 2005.
5. Longley DB, Allen WL and Johnston PG: Drug resistance, predictive markers and pharmacogenomics in colorectal cancer. Biochim Biophys Acta 1766: 184-196, 2006.
6. Lippman SM: The dilemma and promise of cancer chemoprevention. Nat Clin Pract Oncol 10: 523, 2006.
7. Folkman J: Anti-angiogenesis: new concept for therapy of solid tumors. Ann Surg 75: 409-416, 1972.
8. Holash J, Wiegand SJ and Yancopoulos GD: New model of tumor angiogenesis: dynamic balance between vessel regression and growth mediated by angiopoietins and VEGF. Oncogene 18: 5356-5362, 1999.
9. Folkman J: Seminars in Medicine of the Beth Israel Hospital, Boston. Clinical applications of research on angiogenesis. N Engl J Med 333: 1757-1763, 1995.
10. Folkman J: Angiogenesis: an organizing principle for drug discovery? Nat Rev Drug Discov 6: 273-286, 2007.
11. Folkman J: Angiogenesis. Annu Rev Med 57: 1-18, 2006.
12. Folkman J: Tumor angiogenesis: therapeutic implications. N Engl J Med 285: 1182-1186, 1971.
13. Cook KM and Figg WD: Angiogenesis inhibitors: current strategies and future prospects. CA Cancer J Clin 60: 222-243, 2010.
14. Ingham PW, Nakano Y and Seger C: Mechanisms and functions of Hedgehog signalling across the metazoa. Nat Rev Genet 12: 393-406, 2011.
15. Theunissen JW and de Sauvage FJ: Paracrine Hedgehog signaling in cancer. Cancer Res 69: 6007-6010, 2009.
16. Das S, Tucker JA, Khullar S, Samant RS and Shevde LA: Hedgehog signaling in tumor cells facilitates osteoblast-enhanced osteolytic metastases. PLoS One 7: e34374, 2012.
17. Sahebjam S, Siu LL and Razak AA: The utility of hedgehog signaling pathway inhibition for cancer. Oncologist 17: 1090-1099, 2012.
18. Yoshikawa K, Shimada M, Miyamoto H, Higashijima J, Miyatani T, Nishioka M, Kurita N, Iwata T and Uehara H: Sonic hedgehog relates to colorectal carcinogenesis. J Gastroenterol 44: 1113-1117, 2009.
19. Varnat F, Duquet A, Malerba M, Zbinden M, Mas C, Gervaz P and Ruiz i Altaba A: Human colon cancer epithelial cells harbour active HEDGEHOG-GLI signalling that is essential for tumour growth, recurrence, metastasis and stem cell survival and expansion. EMBO Mol Med 1: 338-351, 2009.
20. Mazumdar T, DeVecchio J, Shi T, Jones J, Agyeman A and Houghton JA: Hedgehog signaling drives cellular survival in human colon carcinoma cells. Cancer Res 71: 1092-1102, 2011.
21. Lum L and Beachy PA: The Hedgehog response network: sensors, switches, and routers. Science 304: 1755-1759, 2004.
22. Varjosalo M and Taipale J: Hedgehog: functions and mechanisms. Genes Dev 22: 2454-2472, 2008.
23. Lin JM, Wei LH, Shen AL, Cai QY, Xu W, Li H, Zhan YZ, Hong ZF and Peng J: *Hedyotis diffusa* Willd extract suppresses Sonic hedgehog signaling leading to the inhibition of colorectal cancer angiogenesis. Int J Oncol 42: 651-656, 2013.
24. Auzenne EJ, Klostergaard J, Mandal PK, Liao WS, Lu Z, Gao F, Bast RC Jr, Robertson FM and McMurray JS: A phosphopeptide mimetic prodrug targeting the SH2 domain of Stat3 inhibits tumor growth and angiogenesis. J Exp Ther Oncol 10: 155-162, 2012.
25. Bromberg J and Wang TC: Inflammation and cancer: IL-6 and STAT3 complete the link. Cancer Cell 15: 79-80, 2009.
26. Kusaba T, Nakayama T, Yamazumi K, Yakata Y, Yoshizaki A, Inoue K, Nagayasu T and Sekine I: Activation of STAT3 is a marker of poor prognosis in human colorectal cancer. Oncol Rep 15: 1445-1451, 2006.
27. Franke TF, Kaplan DR, Cantley LC and Toker A: Direct regulation of the Akt proto-oncogene product by phosphatidylinositol-3, 4-bisphosphate. Science 275: 665-668, 1997.
28. Clarke RB: $p27^{KIP1}$ phosphorylation by PKB/Akt leads to poor breast cancer prognosis. Breast Cancer Res 5: 162-163, 2003.
29. Chang F, Lee JT, Navolanic PM, Steelman LS, Shelton JG, Blalock WL, Franklin RA and McCubrey JA: Involvement of PI3K/Akt pathway in cell cycle progression, apoptosis, and neoplastic transformation: a target for cancer chemotherapy. Leukemia 17: 590-603, 2003.

30. Sun D, Liu Y, Yu Q, Zhou Y, Zhang R, Chen X, Hong A and Liu J: The effects of luminescent ruthenium(II) polypyridyl functionalized selenium nanoparticles on bFGF-induced angiogenesis and AKT/ERK signaling. Biomaterials 34: 171-180, 2013.
31. Al-Ansari MM, Hendrayani SF, Tulbah A, Al-Tweigeri T, Shehata AI and Aboussekhra A: $p16^{INK4A}$ represses breast stromal fibroblasts migration/invasion and their VEGF-A-dependent promotion of angiogenesis through Akt inhibition. Neoplasia 14: 1269-1277, 2012.
32. Pratheeshkumar P, Budhraja A, Son YO, Wang X, Zhang Z, Ding S, Wang L, Hitron A, Lee JC, Xu M, Chen G, Luo J and Shi X: Quercetin inhibits angiogenesis mediated human prostate tumor growth by targeting VEGFR-2 regulated AKT/mTOR/P70S6K signaling pathways. PLoS One 7: e47516, 2012.
33. Li W, Tan D, Zhang Z, Liang JJ and Brown RE: Activation of Akt-mTOR-p70S6K pathway in angiogenesis in hepatocellular carcinoma. Oncol Rep 20: 713-719, 2008.
34. Gordaliza M: Natural products as leads to anticancer drugs. Clin Transl Oncol 9: 767-776, 2007.
35. Ji HF, Li XJ and Zhang HY: Natural products and drug discovery. EMBO Rep 10: 194-200, 2009.
36. Lin JM, Wei LH, Xu W, Hong ZF, Liu XX and Peng J: Effect of Hedyotis Diffusa Willd extract on tumor angiogenesis. Mol Med Rep 4: 1283-1288, 2011.
37. Peng J, Chen YQ, Lin JM, Zhuang QC, Xu W, Hong ZF and Sferra TJ: *Patrinia Scabiosaefolia* extract suppresses proliferation and promotes apoptosis by inhibiting STAT3 pathway in human multiple myeloma cells. Mol Med Rep 4: 313-318, 2011.
38. Wei LH, Chen YQ, Lin JM, Zhao JY, Chen XZ, Xu W, Liu XX, Sferra TJ and Peng J: *Scutellaria Barbata* D. Don induces apoptosis of human colon carcinoma cell via activation of the mitochondrion-dependent pathway. J Med Plants Res 5: 1962-1970, 2011.
39. Zheng LP, Chen YQ, Lin W, Zhuang QC, Chen XZ, Xu W, Liu XX, Peng J and Sferra TJ: *Spica Prunellae* extract promotes mitochondrion-dependent apoptosis in a human colon carcinoma cell line. Afr J Pharm Pharmacol 5: 327-335, 2011.
40. Ikeda Y, Murakami A and Ohigashi H: Ursolic acid: an anti- and pro-inflammatory triterpenoid. Mol Nutr Food Res 52: 26-42, 2008.
41. Andersson D, Liu JJ, Nilsson A and Duan RD: Ursolic acid inhibits proliferation and stimulates apoptosis in HT29 cells following activation of alkaline sphingomyelinase. Anticancer Res 23: 3317-3322, 2003.
42. Prasad S, Yadav VR, Sung B, Reuter S, Kannappan R, Deorukhkar A, Diagaradjane P, Wei C, Baladandayuthapani V, Krishnan S, Guha S and Aggarwal BB: Ursolic acid inhibits growth and metastasis of human colorectal cancer in an orthotopic nude mouse model by targeting multiple cell signaling pathways: chemosensitization with capecitabine. Clin Cancer Res 18: 4942-4953, 2012.
43. Pola R, Ling LE, Silver M, Corbley MJ, Kearney M, Pepinsky RB, Shapiro R, Taylor FR, Baker DP and Asahara T: The morphogen Sonic hedgehog is an indirect angiogenic agent upregulating two families of angiogenic growth factors. Nat Med 7: 706-711, 2001.
44. Kujawski M, Kortylewski M, Lee H, Herrmann A, Kay H and Yu H: Stat3 mediates myeloid cell-dependent tumor angiogenesis in mice. J Clin Invest 118: 3367-3677, 2008.
45. Muñoz-Chápuli R, Quesada AR and Angel Medina M: Angiogenesis and signal transduction in endothelial cells. Cell Mol Life Sci 61: 2224-2243, 2004.
46. Chen HX and Cleck JN: Adverse effects of anticancer agents that target the VEGF pathway. Nat Rev Clin Oncol 6: 465-477, 2009.
47. Zangari M, Fink LM, Elice F, Zhan F, Adcock DM and Tricot GJ: Thrombotic events in patients with cancer receiving antiangiogenesis agents. J Clin Oncol 27: 4865-4873, 2009.
48. Higa GM and Abraham J: Biological mechanisms of bevacizumab-associated adverse events. Expert Rev Anticancer Ther 9: 999-1007, 2009.
49. Eikesdal HP and Kalluri R: Drug resistance associated with antiangiogenesis therapy. Semin Cancer Biol 19: 310-317, 2009.
50. Ferrara N, Gerber HP and LeCouter J: The biology of VEGF and its receptors. Nat Med 9: 669-676, 2003.
51. Rak J and Kerbel RS: bFGF and tumor angiogenesis - Back in the limelight? Nat Med 3: 1083-1084, 1997.